Available online at www.sciencedirect.com
ScienceDirect
Optics & Laser Technology 39 (2007) 1135–1139
Optics & Laser Technology
www.elsevier.com/locate/optlastec

High-average-power and high-conversion-efficiency continuous wave mode-locked Nd:YVO_4 laser with a semiconductor absorber mirror

Ji-ying Peng[a,c,*], Jie-guang Miao[a,c], Yong-gang Wang[b], Bao-shan Wang[a,c], Hui-ming Tan[a], Long-sheng Qian[a], Xiao-yu Ma[b]

[a]*Changchun Institute of Optics, Fine Mechanics and Physics, Chinese Academy of Science, Changchun 130022, China*
[b]*Institute of Semiconductors, Chinese Academy of Science, Beijing 100083, China*
[c]*Graduated School of Chinese Academy of Science, Beijing 100039, China*

Received 24 July 2006; received in revised form 1 September 2006; accepted 6 September 2006
Available online 27 October 2006

Abstract

A high-power continuous wave (cw) mode-locked Nd:YVO_4 solid-state laser was demonstrated by use of a semiconductor absorber mirror (SAM). The maximum average output power was 8.1 W and the optic-to-optic conversion efficiency was about 41%. At the maximum incident pump power, the pulse width was about 8.6 ps and the repetition rate was 130 MHz. Experimental results indicated that this absorber was suitable for high power mode-locked solid-state lasers.

Keywords: High-average-power; High-efficiency; CW mode-locked

1. Introduction

Since the first cw mode-locked (CML) solid-state laser with SESAM was demonstrated the mode-locked solid-state lasers were well developed in recent years [1–5]. One of the important frontiers is high average power [6]. Picosecond high-power diode-pumped solid-state lasers with good beam quality are attracting growing interest because of numerous applications in medicine, material processing and nonlinear frequency conversion. The main challenges for high-power lasers were Q-switching instabilities and the SESAM damage. With single LD pumping, one group has achieved 6.2 W average output power with a slope efficiency of 35% and the other group has achieved 5.3 W average output power with a conversion efficiency of 30% [7,8]. The thermal lens of the laser crystal and the SESAM damage were the main reason for the limiting average output power. In this experiment, we used a super SAM as the saturable absorber which had a high damage threshold and we designed the laser cavity elaborately for mitigating the effect of the thermal lens. Finally, we achieved a high average output power of 8.1 W at the maximum incident pump power in CML operation; the optic-to-optic conversion efficiency was about 41%. The nonsaturable losses of the SAM was small and the SAM was not damaged in the experiment.

2. Theoretical discussion about the thermal lens

It is worthwhile to analyze the thermal lens in the Nd:YVO_4 crystal, which affects the output power of the laser and the stability of the resonator. For a laser pumped by a fiber-coupled diode the focal length of the thermal lens f_{th} can be approximately given by [9–11]

$$f_{th} = \frac{\pi K_c \omega_p^2}{P_{ph}(dn/dT)} \frac{1}{1-\exp(-\alpha l)}.$$

Where K_c is the thermal conductivity, ω_p is the average pump size in the laser crystal, P_{ph} is the fraction of pump power that results in heating, dn/dT is the thermo-optic coefficient, α is the absorption coefficient, l is the length of the laser crystal. Usually about 24% of the pump power is

*Corresponding author. Changchun Institute of Optics, Fine Mechanics and Physics, Chinese Academy of Science, Changchun 130022, China.
E-mail address: jiyingpeng111@163.com (J.-y. Peng).

0030-3992/$ - see front matter © 2006 Elsevier Ltd. All rights reserved.
doi:10.1016/j.optlastec.2006.09.006

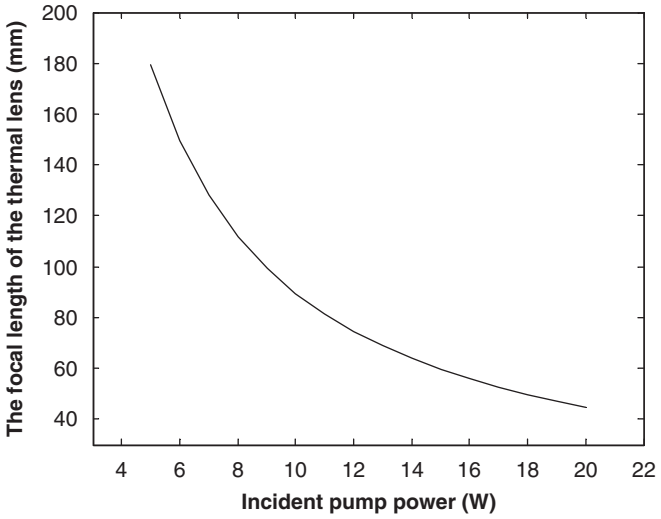

Fig. 1. The calculated focal length of the thermal lens as a function of the incident pump power.

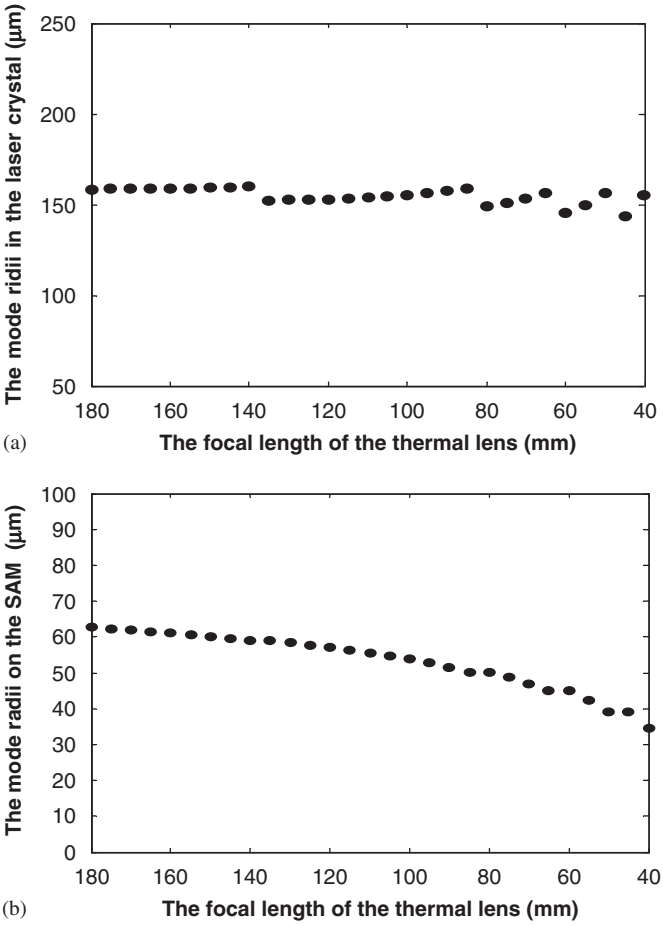

Fig. 2. (a) The calculated mode radii in the laser crystal at different focal length of the thermal lens; (b) the calculated mode radii on the SAM at different focal length of the thermal lens.

changed to heat. The focal length of the thermal lens is estimated by using the following parameters: $K_c = 0.051\,\mathrm{W/K\,cm}$, $\mathrm{d}n/\mathrm{d}T = 3.0 \times 10^{-6}/\mathrm{K}$, $\omega_p = 0.2\,\mathrm{mm}$, $\alpha = 10\,\mathrm{cm}^{-1}$, and $l = 5\,\mathrm{mm}$. The calculated focal length of the thermal lens as a function of the absorbed pump power was shown in Fig. 1. The focal length of the thermal lens was found to be about 45 mm at 20 W pump power. Considering the thermal lens effect, we designed a thermal-stable cavity. The cavity was designed to easily allow mode matching with the pump beam and to provide the proper spot size on the SAM. The mode radii in the laser crystal was about 140–160 μm (0.7–0.8 times of the pump size); the mode radii on the SAM was approximately 30–60 μm. The mode radii were calculated by the laser transfers matrix. Fig. 2 showed the mode radii at different focal length. From Fig. 1 we knew that when the incident pump power was increased, the thermal lens effect became more serious. In this case, to keep precise mode-matching and achieve high conversion efficiency, the distance between the mirror M2 and the SAM should be changed slightly. The distance was controlled to be 102–98 mm. For obviously revealing the mode radii variation with the distance, the 1 mm changing pace was taken. One step occurred in the curves of Fig. 2 when the distance changed 1 mm.

3. Experimental setup and results

The SAM was grown on GaAs substrate by metal-organic chemical-vapor deposition. The SAM consisted of 22 pairs of GaAs/AlAs quarter-wave Bragg layers with high reflectivity of 99.5% at lasing wavelength of 1064 nm and a 15-nm relaxed $In_{0.3}Ga_{0.7}As$ single quantum well (embedded in the topmost layer of the Bragg stack) for achieving saturable absorption at 1064 nm. The Bragg layers and the $In_{0.3}Ga_{0.7}As$ absorber were grown at temperatures of 720 and 500 °C, respectively. For getting a high damage threshold, the SAM was coated with three pairs of SiO_2/Al_2O_3 as the protective film and the reflectivity was about 50%. The $In_{0.3}Ga_{0.7}As$ absorber was grown at 500 °C low temperature for a fast recovery time. The structure is shown in detail in Fig. 3.

The cavity configuration was shown in Fig. 4. The Nd^{3+} concentration of the laser crystal was 0.5 at%, and its length was 5 mm. The laser crystal was wrapped with indium foil and mounted in a copper block cooled by a thermo-electric cooler. One side of the laser crystal was coated antireflection for 808 nm ($T > 98\%$) pump wavelength and high reflection ($R > 99.8\%$) for the 1064 nm lasing radiation, the other side was coated antireflection for 1064 nm. The pump source was 20 W fiber-coupled laser diode with a core diameter of 0.4 mm and a numerical aperture of 0.22. The central wavelength of the LD was 810.2 nm at 25 °C and can be tuned by changing the working temperature of the LD to match the best absorption of the laser crystal. The fiber output was focused into the laser crystal and the pump spot radii were about 200 μm. The resonator consisted of two highly reflective (at 1064 nm) mirrors, M1 and M2; one partially reflective (PR) mirror, output coupler (OC); a laser crystal; and a SAM. OC is a flat mirror; the radii of curvature for

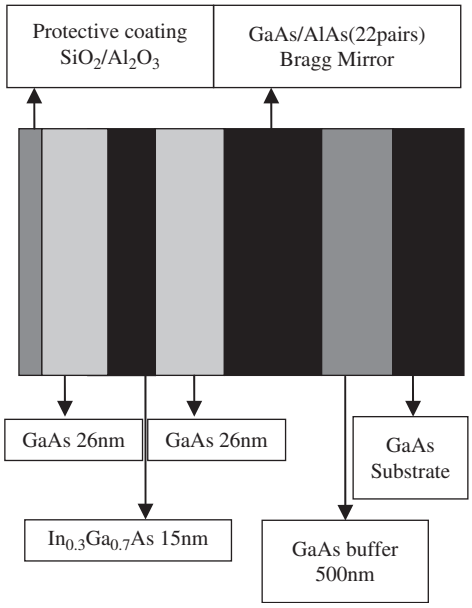

Fig. 3. The scheme of the SAM structure.

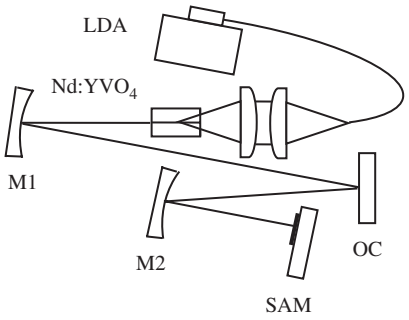

Fig. 4. Configuration of the mode-locked Nd:YVO_4 laser with a SAM.

M1 and M2 are 500 and 200 mm, respectively. OC had a reflectivity of 90% at 1064 nm, giving a total output coupling of 19%. The total cavity length was about 1145 mm. M1 and M2 were separated by about 740 mm. The mode radii in the crystal was about 140–160 μm; The mode radii on the SAM was approximately 30–60 μm. The SAM was simply mounted on a copper heat sink, but no active cooling was applied.

To optimize the laser output we selected three OCs, the reflectivity were 80%, 90%, and 95%, respectively. Using the 80% reflectivity coupler, we achieved the highest average output power of 8.9 W; however the CML threshold was too high. Till 14.7 W pump power, the QML state was transformed into a CML state. A maximum average output power of 6.2 W was obtained with the 95% reflectivity coupler, it was relatively low. For the 90% reflectivity coupler, both the average output power and the CML threshold were moderate for this laser. So in our opinion the 90% reflectivity coupler was the best choice.

The behavior of laser average output power as a function of the incident pump power was investigated as shown in

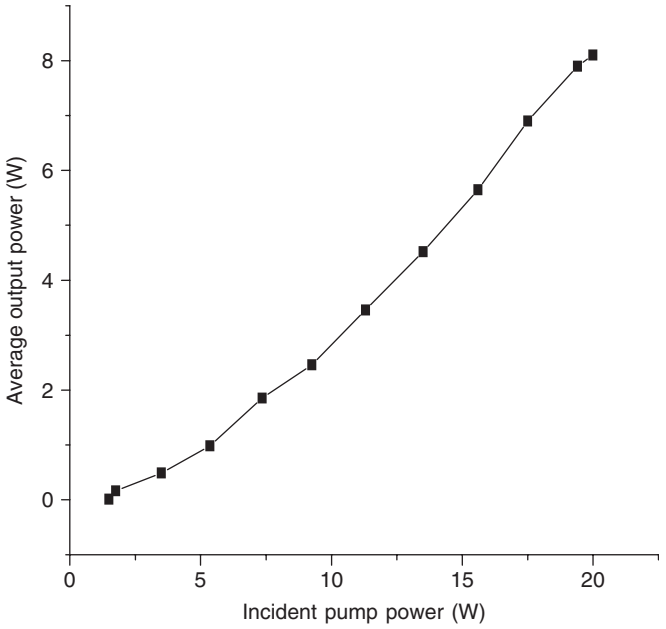

Fig. 5. The average output power as a function of incident pump power.

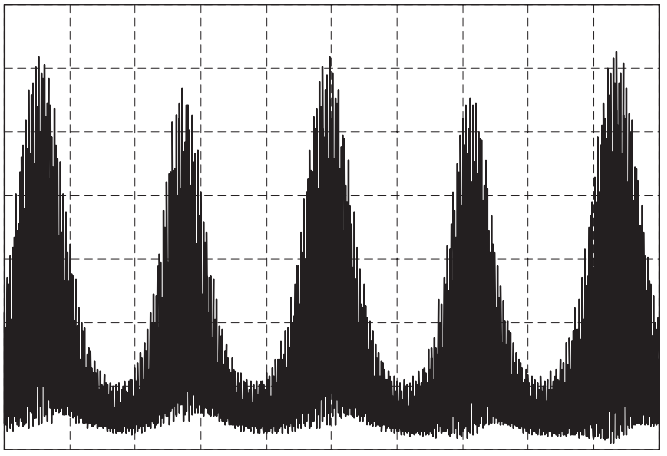

Fig. 6. Q-switched mode-locked pulse train (2 μs/div).

Fig. 5. The oscillation threshold was about 1.55 W. The low threshold indicated that the SAM did not induce significant nonsaturable losses. Near oscillation threshold the output was effectively cw; slightly increasing the pump power initiated a Q-switched mode-locked (QML) state. The temporal behavior of laser pulses was recorded by a fast response InGaAs photodiode with a time resolution of 0.5 ns and a LeCroy oscilloscope (9361C). The QML pulse train was shown in Fig. 6. The repetition rate of the Q-switched envelope increased from 125 to 330 kHz as the incident pump power increased from 3 to 8 W. The pulse width of the Q-switched envelope was about 2 μs. When the pump power increased to be about 8 W, the QML state is transformed into a CML state. At 8 W pump power the average output power was about 2.15 W. Figs. 7 and 8 showed the CML pulse train in different time division, respectively. The repetition rate was about 130 MHz.

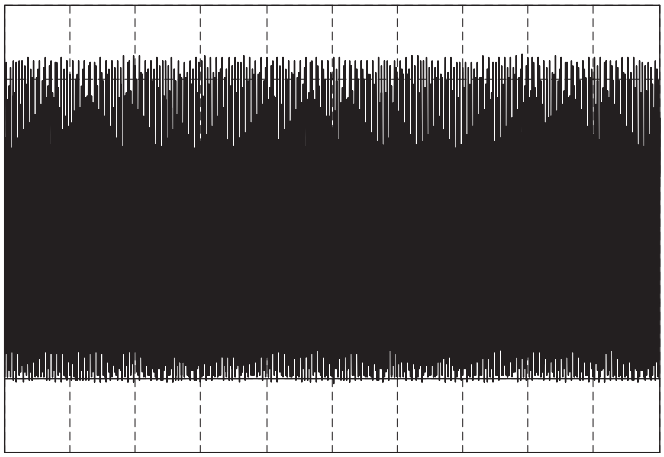

Fig. 7. CW mode-locked pulse train (2 μs/div).

Fig. 8. CW mode-locked pulse train (10 ns/div).

At the maximum incident pump power of 20 W, 8.1 W average output power was obtained. The optical–optical conversion efficiency was about 41%. At 20 W pump power, the pulse width of the CML laser output was measured by a homemade autocorrelator with a 3 mm long KTP crystal under type-II phase-matched second-harmonic interaction in a collinear configuration. The autocorrelation trace was shown in Fig. 9. The pulse width was about 8.6 ps by assuming a Gaussian pulse shape. The optical spectrum was measured by a Spectrum Analyzer (AQ 6317B) and was shown in Fig. 10. The spectrum was centered at 1064.4 nm with a FWHM bandwidth of about 0.40 nm with a slight asymmetric spectral distribution. In our opinion, the etalon effect from the two end surfaces of the laser crystal led to the asymmetric spectral profile. The time-bandwidth product was calculated to be 0.91, indicating a chirped pulse. Probably, it was the SAM recovery time or the crystal dispersion that limited the mode-locked pulse. For measuring the laser beam quality factor M^2 the beam was focused with a plano-concave lens ($f = 200$ mm). The laser beam quality factor M^2 was measured to be about 1.41 for the sagittal plane and 1.45 for the tangential plane by the knife-edge technique [12].

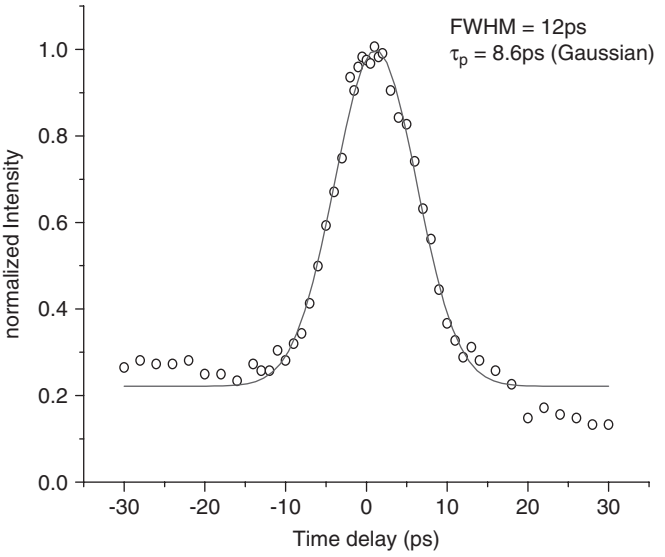

Fig. 9. Autocorrelation trace of the output pulses from the cw mode-locked Nd:YVO_4 laser.

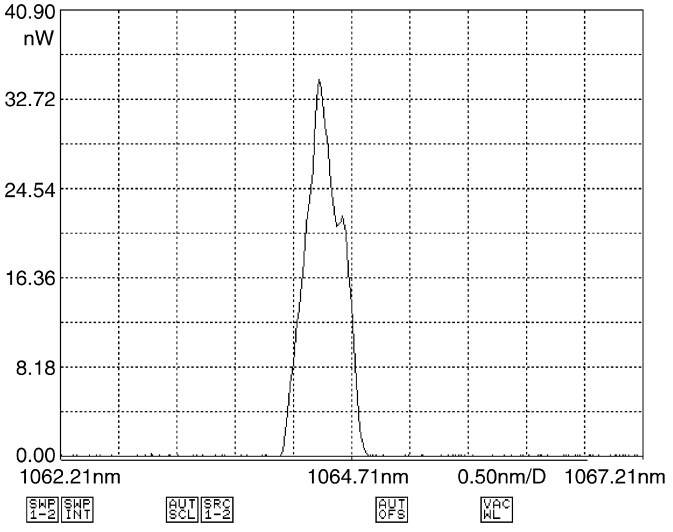

Fig. 10. The optical spectrum of the CW mode-locked laser output.

No damage to the SAM was observed over several hours of operation, which indicated a high damage threshold of the super SAM. The average output power always increased along with the increased incident pump power and the optical–optical conversion efficiency (41%) was relatively high, which indicated a logical cavity design.

4. Conclusion

We have demonstrated a high-power diode-end-pumped cw mode-locked Nd:YVO_4 laser by using a semiconductor absorber mirror as the saturable absorber. Considering the thermal lens effect, we elaborately designed the laser cavity, and obtained 8.1 W of average output power in 8.6 ps Gaussion pulses at a repetition rate of 130 MHz. The maximum optic-to-optic conversion efficiency was about

41%. The Q-switching instability was well suppressed and the cw mode-locked pulse train was stable. The low insertion loss and high damage threshold indicated that the SAM is suitable for high power mode-locked lasers.

References

[1] Keller U, Miller DAB, Boyd GD, Chiu TH, Ferguson JF, Asom MT. Solid-state low-loss intracavity saturable absorber for Nd:YLF lasers: an antiresonant semiconductor Fabry-Perot saturable absorber. Opt Lett 1992;17:505–7.

[2] Paschotta R, Au JA, Spuhler GJ, Genoud FM, Hovel R, Moser M, et al. Diode-pumped passively mode-locked lasers with high average power. Appl Phys B 2000;70:S25–31.

[3] Zhang B, Li G, Chen M, Zhang Z, Wang Y. Passive mode locking of a diode-end-pumped Nd:$GdVO_4$ laser with a semiconductor saturable absorber. Opt Lett 2003;28:1829–31.

[4] He J, Fan Y, Du J, Wang Y, Liu S, Wang H, et al. 4 ps passively mode-locked Nd:$Gd_{0.5}Y_{0.5}VO_4$ laser with a semiconductor saturable absorber mirror. Opt Lett 2004;29:2803–5.

[5] Du J, Liang X, Wang Y, Su L, Feng W, Dai E, et al. 1 ps passively mode-locked laser operation of Na,Yb:CaF_2 crystal. Opt Express 2005;13:7970–5.

[6] Keller U. Recent developments in compact ultrafast lasers. Nature 2003;424:831–8.

[7] Jabczynski JK, Zendaian W, Kwiatkowski. Diode pumped cw mode-locked Nd:YVO_4 laser. Proc SPIE 2005;5958:5958201–6.

[8] Cai Z, Wen W, Wang Y, Zhang Z, Ma X, Ding X, et al. 5.3 W Nd:YVO_4 passively mode-locked laser by a novel semiconductor saturable absorber mirror. Chinese Opt Lett 2005;3:342–4.

[9] Innocenzi M, Yura H, Fincher C, Fieids R. Thermal modeling of continuous-wave end-pumped solid-state lasers. Appl Phys Lett 1990;56:1831–3.

[10] Song F, Zhang C, Ding X, Xu J, Zhang G, Leigh M, et al. Determination of thermal focal length and pumping radius in gain medium in laser-diode-pimped Nd:YVO_4 lasers. Appl Phys Lett 2002;81:2145–7.

[11] Peng X, Asundi A, Chan Y, Xiong Z. Heating measurements in diode-end-pumped Nd:YVO_4 laser. Opt Eng 2001;40:1100–5.

[12] Siegman A, Sasnett M, Johnston T. Choice of clip levels for beam width measurements using knife-edge techniques. IEEE J Quantum Electron 1991;27:1098–104.